2016

The Influence of Non-Condensable Gases on the Thermal-Acoustic Behavior of Household Refrigerators

Rodolfo da Silva Espíndola
Federal University of Santa Catarina, Brazil, rodolfo@polo.ufsc.br

Fernando Testoni Knabben
Federal University of Santa Catarina, Brazil, fernandok@polo.ufsc.br

Claudio Melo
Federal University of Santa Catarina, Brazil, melo@polo.ufsc.br

The Influence of Non-condensable Gases on the Thermal-acoustic Behavior of Household Refrigerators

Rodolfo S. ESPÍNDOLA, Fernando T. KNABBEN, Cláudio MELO*

POLO – Research Laboratories for Emerging Technologies in Cooling and Thermophysics
Department of Mechanical Engineering, Federal University of Santa Catarina, Florianópolis, SC, Brazil,
+55 48 3234 5691, melo@polo.ufsc.br

* Corresponding Author

ABSTRACT

In refrigeration systems with evaporating pressure lower than atmospheric pressure, air from the ambient can infiltrate into the circuit through small leaks in the suction line. Additionally, if a problem occurs during the evacuation process on the production line, residual air might be left inside the circuit. This paper reports an experimental study on the influence of non-condensable gases on the thermal-acoustic behavior of a household refrigeration system. Controlled amounts of nitrogen were injected into the system through a purpose-built device. Steady-state energy consumption tests were carried with different nitrogen mass fractions inside the circuit at compressor speeds of 2500, 3000 and 4000 RPM. In addition, acceleration signals were captured by an accelerometer installed at the evaporator inlet simultaneously with images of the flow at the capillary tube inlet. It was found that for very low nitrogen mass fractions the system performance was not affected and in some cases was slightly improved. However, for high nitrogen mass fractions, large fluctuations in the flow pattern at the capillary tube inlet and in the acceleration readings were observed resulting in a worse system performance. Furthermore, a high sub-cooling degree at the filter dryer was a strong evidence of the presence of non-condensable gases.

1. INTRODUCTION

In refrigeration systems with evaporating pressure lower than atmospheric pressure (e.g. refrigerators operating with isobutane), air from the external environment can infiltrate into the circuit through small leaks in the suction line. Additionally, if a problem occurs during the evacuation process on the production line, residual air might be left inside the circuit. Since air is composed mostly of nitrogen, a gas with a very low boiling point, it remains in the vapor phase throughout the refrigeration circuit, which means it does not condense. A non-condensable gas can adversely affect the system operation, reducing its energy efficiency and increasing the flow noise level.

According to Cecchinato *et al.* (2007), if a liquid receiver is located at the condenser outlet, a liquid seal is formed and all non-condensable gases become trapped inside the condenser. The area occupied by these gases in the condenser is not available for refrigerant heat transfer. In addition, the internal heat transfer coefficient is reduced, since the gas does not condense. In order to compensate the reduction in the heat exchange area and the heat transfer coefficient, the temperature difference between the refrigerant and the air has to increase, which causes an increase in the discharge pressure and in the power required by the compressor, resulting in a lower coefficient of performance (COP).

In the absence of a liquid receiver at the condenser outlet, no trap is formed and the non-condensable gases can freely circulate through the circuit. A gaseous mixture of refrigerant vapor and non-condensable gas can then enter the capillary tube and, since the temperature of the suction line in contact with the capillary tube is not sufficiently low, these vapor mixture cannot collapse. Thus, the capillary tube gets choked, causing fluctuations in the flow and reducing the refrigerant mass flow rate. Furthermore, the discharge pressure increases due to the addition of the partial pressure of non-condensable gases to the condensing pressure. The combination of these factors reduces the system COP.

There are few reports in the open literature on this topic. In fact, the only study found was that performed by Cechinatto *et al.* (2007), who experimentally investigated the effect of non-condensable gases in household refrigeration by injecting small amounts of air into the refrigeration circuit. The doping procedure was simple and consisted of varying the air volume in the plunger of a syringe. An all-refrigerator and an upright freezer were tested under steady-state and cyclic conditions. However, their analysis was restricted to thermodynamic parameters. In this context, the aim of the study presented herein was to extend the analysis of the effect of non-condensable gases in household refrigeration by visualizing the flow pattern at the capillary tube inlet and capturing acceleration signals at the evaporator inlet. In addition, an accurate device to inject controlled amounts of nitrogen into the system was developed. Furthermore, a variable speed compressor was used to allow the operation under different conditions and to create an imbalance between the compressor and the capillary tube.

2. EXPERIMENTAL SETUP

2.1 Refrigerator

A bottom-mount frost-free refrigerator was used in the experiments, with a 120-liter freezer placed below a 302-liter fresh-food compartment (see Figure 1). The refrigeration system has a reciprocating variable speed compressor and operates with 56 g of isobutane. The evaporator is of the finned-tube type, subjected to forced convection by an axial fan which blows the total airflow into a plenum, where a damper directs part to the freezer and part to the fresh-food compartment. The condenser is of the wire-and-tube type, with 25 rows, located at the refrigerator rear wall.

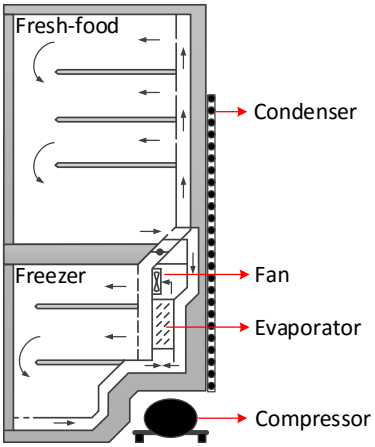

Figure 1: Refrigerator

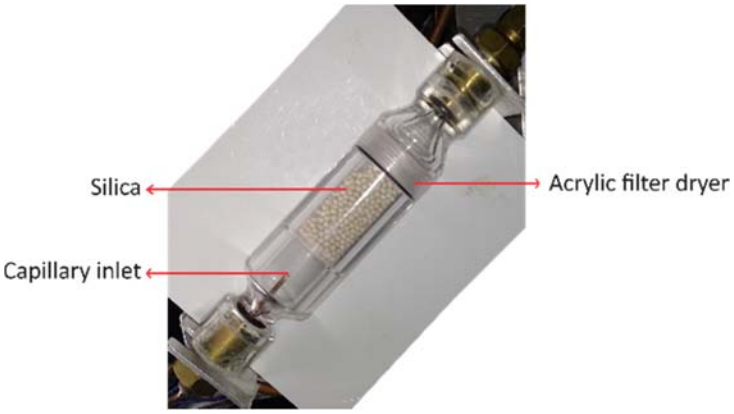

Figure 2: Acrylic filter dryer

The flow pattern at the capillary tube inlet can be strongly affected by the presence of non-condensable gases. In order to visualize this effect, the original filter dryer was replaced by an acrylic-made replica (see Figure 2), and images were recorded by a high-speed camera, model i-SPEED TR, manufactured by Olympus.

In order to obtain the temperature profile along the condenser, 25 T-type thermocouples (uncertainty of ±0.2 ºC) were installed on each row of the condenser. Since the presence of non-condensable gases tends to increase the sub-cooling degree at the condenser outlet, it is very important to monitor its whole extension. With regard to the air temperature inside the cabinets, five thermocouples were installed in the fresh-food compartment (two in the cellar compartment and three in the geometric center of the shelves) and three other thermocouples were uniformly placed in the freezer. The electrical parameters, such as voltage, current and power were measured by transducers with an uncertainty of ±0.1% of the readings.

To monitor the refrigerant pressure, absolute pressure transducers (uncertainty of ± 0.01 bar) were installed at the compressor suction and discharge ports, as well as in the filter dryer. The refrigerant sub-cooling (SUB) at the filter dryer inlet was then calculated by the following equation:

$$SUB = T_{sat}\left(P_{dryer}\right) - T_{dryer} \tag{1}$$

where $T_{sat(P_{dryer})}$ is the refrigerant saturation temperature considering the filter dryer pressure and T_{dryer} is the refrigerant temperature at the filter dryer.

In addition, an accelerometer, model CCLD 4533-B, manufactured by Brüel & Kjær, was strategically installed at the evaporator inlet, in order to monitor the vibration in the tube due to the expansion process at the capillary tube outlet.

2.2 Doping device

A doping device was developed to accurately inject small amounts of nitrogen into the refrigeration circuit (see Figure 3). The injection process comprises the following steps: first, the apparatus must be evacuated and then valve V_1 must be opened to inject nitrogen into the device, until a predefined initial pressure is reached. Then valve V_1 must be closed and after a steady-state condition is achieved the initial pressure and temperature inside the device are recorded (p_i and T_i, respectively). After that, valve V_2 must be opened in order to release nitrogen to the refrigeration system until the desired final pressure is reached. The valve V_2 must be closed and the final pressure and temperature are recorded (p_f and T_f, respectively). The nitrogen mass injected (m_{nit}) is calculated from Equation (2), assuming an ideal gas behavior, where V_{dev} stands for the inner volume of the device (previously measured by a similar method, Gonçalves, 2004) and R is the specific gas constant of nitrogen.

$$m_{nit} = \left(\frac{p_i}{T_i} - \frac{p_f}{T_f} \right) \frac{V_{dev}}{R} \tag{2}$$

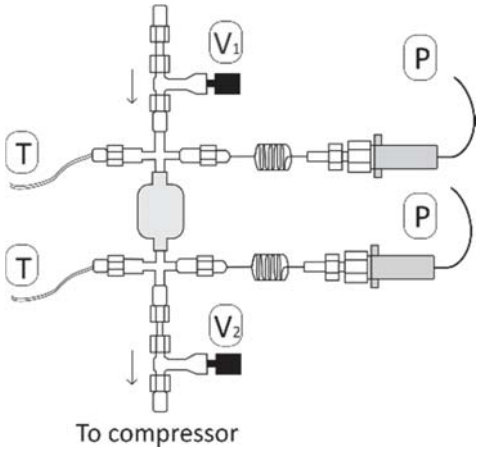

Figure 3: Doping device

3. TESTING PROCEDURE

In order to evaluate the effect of non-condensable gases on the performance of the refrigerator, energy consumption tests were carried out according to the steady-state methodology proposed by Hermes *et al.* (2013). Reverse leakage tests (Gonçalves *et al.*, 2000) were carried out to determine the global thermal conductances of the compartments, parameters which are required to calculate the thermal load and the energy consumption. Further details are shown in the following sections.

3.1 Reverse heat leakage tests

Reverse heat leakage tests were carried out in a climate chamber at 15 ºC. PID-driven electric heaters were uniformly distributed inside the compartments in order to increase their temperatures, thereby creating a heat flux from the internal compartments to the external ambient. During the tests, only the evaporator fan was kept running. Six tests were performed, varying the damper positions (open and closed) and the temperatures of the fresh-food and freezer compartments, as shown in Table 1.

Table 1: Reverse heat leakage test data

Damper	Test	T_a [°C]	T_{ff} [°C]	T_{fz} [°C]	W_f [W]	W_{ff} [W]	W_{fz} [W]
Open	1	15.0	47.7	54.7	8.6	9.4	42.0
	2	14.9	51.9	60.1	8.6	10.7	49.2
	3	15.2	60.0	59.9	8.5	44.4	24.8
Closed	4	15.1	35.0	57.8	8.6	14.5	24.8
	5	15.1	44.8	60.0	8.6	26.0	25.1
	6	15.0	60.0	39.9	8.7	48.0	5.0

The thermal conductance of the freezer and the fresh-food compartments (UA_{fz} and UA_{ff}) were calculated by adjusting the equation of the energy balance in the refrigerator, expressed by Equation (3), based on experimental data shown in Table 1. Thermal conductances of 0.66 W/K and 1.03 W/K were obtained for the freezer and fresh-food compartments, respectively.

$$UA_{fz}\left(T_{fz}-T_a\right)+UA_{ff}\left(T_{ff}-T_a\right)-\left(W_{f,e}+W_{fz}+W_{ff}\right)=0 \tag{3}$$

where T_{fz} is the average temperature of air in the freezer compartment, T_{ff} is the average temperature of the air in the fresh-food compartment, T_a is the ambient temperature, W_{fz} is the heat generated in the freezer, W_{ff} is the heat generated in the fresh-food compartment and $W_{f,e}$ is the evaporator fan power.

3.3 Steady-state energy consumption tests

The energy consumption tests were carried out according to the steady-state methodology proposed by Hermes *et al.* (2013). In this methodology, the system is kept running under steady-state conditions through PID-driven electric heaters strategically placed inside the fresh-food and freezer compartments, so that the excess of cooling capacity is overridden by heat generation inside the cabinets. During the tests, the thermostat must be deactivated while the damper is fixed at a predefined position. In order to determine the refrigerator energy consumption, the cabinet thermal load (Q_t) must first be calculated through the following equation:

$$Q_t = UA_{fz}\left(T_a-T_{fz}\right)+UA_{ff}\left(T_a-T_{ff}\right)+W_{f,e} \tag{4}$$

The cooling capacity (Q_e) is obtained by taking into account the thermal load and the heaters power dissipation:

$$Q_e = Q_t + W_{fz} + W_{ff} \tag{5}$$

When the refrigerator operates according to a cycling pattern, the energy transferred into the refrigerated compartments during the whole cycle (time-on plus time-off) must be removed by the cooling system in the time-on period. Thus, the compressor runtime (τ), defined as the ratio between time-on and the total cycle time, can be derived from an energy balance over a whole cycle as follows:

$$Q_e t_{on} = \left[UA_{fz}\left(T_a-T_{fz}\right)+UA_{ff}\left(T_a-T_{ff}\right)\right]\left(t_{on}+t_{off}\right)+W_{f,e}t_{on} \tag{6}$$

resulting in:

$$\tau \equiv t_{on}/\left(t_{on}+t_{off}\right) \cong \left(Q_t-W_{f,e}\right)/\left(Q_e-W_{f,e}\right) \tag{7}$$

Hence, the monthly energy consumption (EC) can be calculated as follows:

$$EC = 0.72\tau\left(W_k+W_{f,e}\right) \tag{8}$$

where W_k is the compressor power and the 0.72 coefficient is a conversion factor from [W] to [kWh/month].

3.3 Acceleration signal and image recordings

After performing a steady-state energy consumption test, with all variables stabilized, data were acquired from the accelerometer during 30 s. Simultaneously, images of the flow at the capillary tube inlet were recorded by the high-speed camera at 180 frames per second. The images were played at a rate of 30 frames per second, which provided a playback speed six times slower than real time and allowed an easier analysis of the flow. The accelerometer data was synchronized with the flow images, so that the vibration captured at the evaporator inlet could be associated with the flow pattern at the capillary tube inlet.

4. RESULTS AND DISCUSSIONS

In all energy consumption tests, the ambient temperature was kept at 32 ºC, the fresh-food temperature at 5 ºC and the freezer temperature at -18 ºC. Tests were carried out at three different compressor speeds: 2500, 3000 and 4000 RPM and the results are shown in Tables 2 to 4.

Table 2: Results obtained at 2500 RPM

2500 RPM	Unit	Baseline	Test 1	Test 2	Test 3	Test 4	Test 5	Test 6
Nitrogen mass fraction	-	0	0.07	0.14	0.21	0.28	0.36	0.53
Compressor power	W	66.9	66.6	63.7	66.6	66.4	65.6	64.3
Cooling capacity	W	106.9	109.2	103.6	107.5	98.7	97.9	90.6
Run-time	%	63.1	61.6	64.4	62.7	68.9	69.0	74.9
Energy consumption	kWh/month	34.79	33.76	33.96	34.36	37.63	37.24	38.48
Discharge pressure	bar	6.17	6.32	6.34	6.64	6.76	6.94	7.23
Suction pressure	bar	0.63	0.61	0.58	0.60	0.60	0.58	0.56
Mass flow rate	kg/h	1.54	1.50	1.37	1.43	1.42	1.37	1.27
Sub-cooling	°C	1.6	7.2	11.3	13.0	14.7	16.3	17.9

Table 3: Results obtained at 3000 RPM

3000 RPM	Unit	Baseline	Test 1	Test 2	Test 3	Test 4	Test 5	Test 6
Nitrogen mass fraction	-	0	0.07	0.14	0.21	0.28	0.36	0.53
Compressor power	W	81.1	78.6	75.7	72.6	75.9	74.3	72.9
Cooling capacity	W	121.0	117.5	113.1	109.8	106.4	103.2	101.5
Run-time	%	55.1	56.7	59.3	61.5	63.2	65.1	66.1
Energy consumption	kWh/month	35.99	36.00	36.36	36.41	38.91	38.50	39.15
Discharge pressure	bar	6.45	6.56	6.63	6.73	6.98	7.10	7.41
Suction pressure	bar	0.61	0.58	0.55	0.52	0.56	0.54	0.53
Mass flow rate	kg/h	1.78	1.68	1.56	1.44	1.52	1.46	1.37
Sub-cooling	°C	2.0	7.5	11.6	13.9	15.6	17.1	18.6

Table 4: Results obtained at 4000 RPM

4000 RPM	Unit	Baseline	Test 1	Test 2	Test 3	Test 4	Test 5	Test 6
Nitrogen mass fraction	-	0	0.07	0.14	0.21	0.28	0.36	0.53
Compressor power	W	103.7	101.3	95.7	92.0	88.3	89.6	92.1
Cooling capacity	W	136.4	137.3	127.4	115.6	108.7	109.3	110.8
Run-time	%	48.5	48.0	52.1	57.9	61.7	61.4	59.8
Energy consumption	kWh/month	39.53	38.35	39.48	42.31	43.44	43.82	43.60
Discharge pressure	bar	6.81	6.94	6.96	7.00	7.08	7.29	7.77
Suction pressure	bar	0.54	0.53	0.49	0.46	0.43	0.44	0.46
Mass flow rate	kg/h	2.00	1.94	1.77	1.62	1.51	1.53	1.55
Sub-cooling	°C	2.8	8.0	12.2	15.3	16.8	17.9	20.1

As previously discussed, an increase in the nitrogen mass can choke or clog the capillary tube due to the entry of a gaseous mixture composed by refrigerant vapor and nitrogen. This contributed to a condenser flooding and led to a progressive increase in the discharge pressure, as can be observed in Figure 4a. As a consequence, the evaporator was starved of refrigerant and the suction pressure decreased.

As the compressor pressure ratio increased, the specific work of compression also increased. On the other hand, the capillary tube clogging effect and the reduction in the suction pressure caused a reduction in the mass flow rate. When comparing the tests with 0.53% of nitrogen to the baseline tests, reductions of 17.5%, 23.0% and 22.5% in the mass flow rate were observed at 2500, 3000 and 4000 RPM, respectively. Therefore, since the compression power is dependent on both the specific work of compression and mass flow rate, a reduction in the compressor power was observed as the nitrogen mass fraction increased. As the mass flow rate decreased, the cooling capacity also decreased. To compensate for this effect, the compressor had to run for a longer period, which explains the runtime increase.

The energy consumption is dependent on the aforementioned parameters. Figure 4b shows the energy consumption results at all compressor speeds. It can be noticed that when the nitrogen mass fraction was very low the system performance was not affected, and actually, there was even a slight improvement in the performance compared to the baseline case. It might seem odd, but Cecchinato *et al.* (2007) also observed this behavior in their experiments. Since the capillary tube is a fixed expansion device, it can operate better under certain conditions than others. Therefore, depending on the operating conditions, a small amount of nitrogen can slightly increase the capillary tube restriction and increase the system performance. However, when the concentration of nitrogen exceeds certain limits, clogging of the capillary tube becomes too detrimental. In the tests at 2500 and 3000 RPM, for example, when the nitrogen mass fraction was 0.28%, the refrigerator energy consumption was about 8% higher than that of the baseline test. At 4000 RPM, when the nitrogen mass fraction was 0.21%, the refrigerator energy consumption was about 7% higher than that of the baseline case.

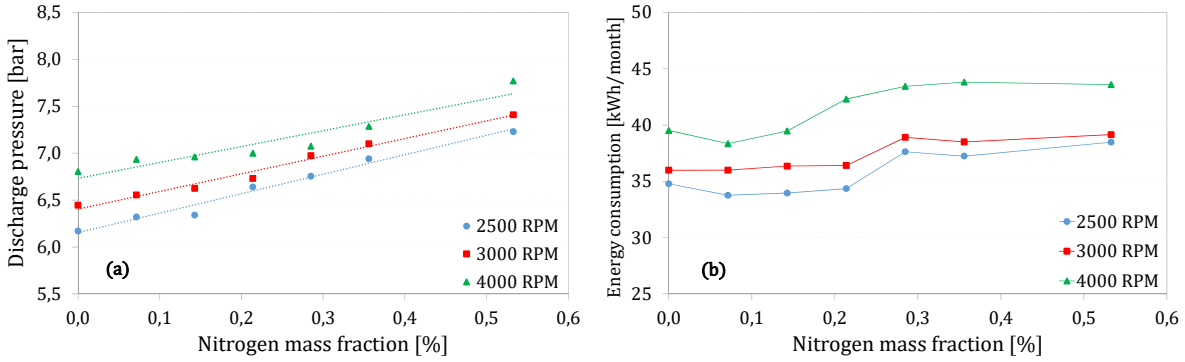

Figure 4: (a) Discharge pressure and (b) energy consumption as a function of nitrogen mass fraction

It can be noted that the effect of non-condensable gases varies for different refrigeration system and components. On changing the compressor speed from 2500 to 4000 RPM, for example, the system was more affected at lower concentrations of nitrogen, which is consistent with the above statements. The higher the compressor speed, the lower the restriction of the expansion device must be in order to optimize the performance. Again considering that the capillary tube is a fixed expansion device, it seems to be better sized for 4000 RPM than for lower compressor speeds. Hence, the clogging of the capillary tube was more detrimental in this case. However, when higher concentrations of nitrogen were applied the system was penalized to a much greater extent at all compressor speeds.

A high sub-cooling degree is a strong evidence of the presence of non-condensable gases, as shown in Figure 5a. For the tests with 0.53% of nitrogen, for example, sub-cooling degrees of 17.9, 18.6 and 20.9 ºC were calculated at compressor speeds of 2500, 3000 and 4000 RPM, respectively. Figure 5b shows the tube wall temperatures from the compressor discharge until the filter dryer for three tests at 4000 RPM: baseline, 0.28% and 0.53% of nitrogen. It was observed that as the nitrogen mass fraction increased, the saturation temperature in the condenser increased, as a

result of the discharge pressure increase. It was also noted that the higher the nitrogen mass fraction the smaller is the area of the condenser used for latent heat transfer.

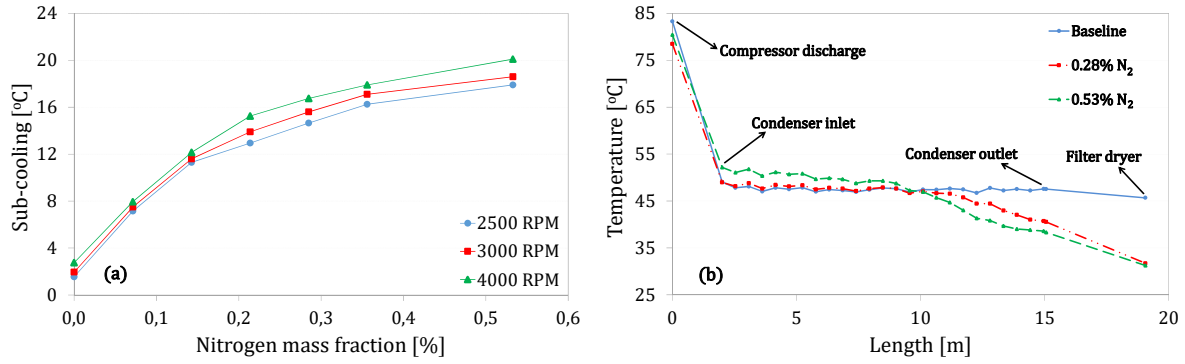

Figure 5: (a) Sub-cooling as a function of nitrogen mass fraction and (b) discharge line temperature profile

Three different behaviors were observed in the analysis of the flow pattern at the capillary tube inlet. The first is shown in Figure 7 for the baseline test at 2500 RPM. Even though the system was operating under steady-state conditions, a few fluctuations were observed at the capillary tube inlet. Most of the time, a high liquid level was observed with a vapor vortex entering the capillary tube (Figure 7a). However, sometimes the vortex suddenly disappeared (Figure 7b) and then reappeared within a very short time (Figures 7c and 7d), causing the acceleration spikes shown in Figure 6a.

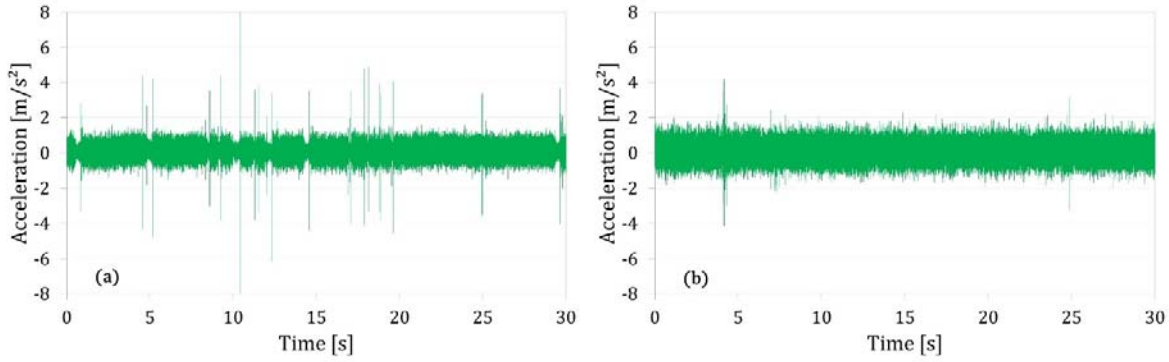

Figure 6: Acceleration data at 2500 RPM: (a) baseline test and (b) 0.07% of nitrogen

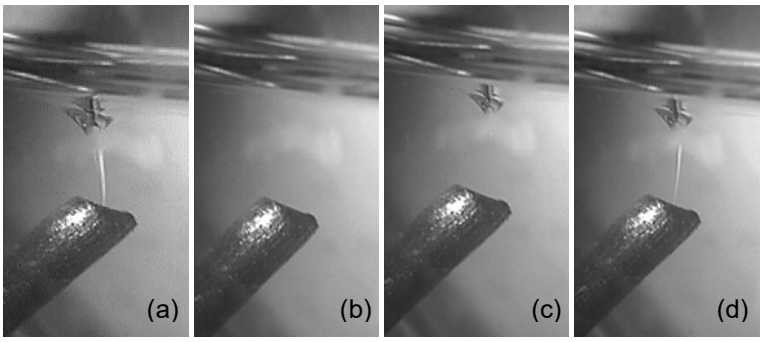

Figure 7: Filter dryer images: baseline test at 2500 RPM

The second behavior is exemplified by the test with 0.07% of nitrogen at 2500 RPM. This case was very similar to the baseline, and there was predominantly liquid with a vapor vortex. The flow, in turn, was more constant and fluctuations were barely seen. Thus, a reduction in the acceleration spikes was registered (see Figure 6b). A small amount of nitrogen optimized the capillary tube flow, which was not perfectly sized for this operating condition, as previously mentioned.

The third case, represented by the test with 0.53% of nitrogen at 2500 RPM, occurred at higher nitrogen mass fractions. An intermittent acceleration pattern was registered, as shown in Figure 8. Figure 9 shows the moments of 10 and 25 s, where it was observed that the liquid level was very low and there was predominantly a gaseous mixture entering the capillary tube. This partially clogged the capillary tube and consequently reduced the mass flow rate and the expansion noise. Higher accelerations, however, were captured when the liquid level was higher, as observed at the moments of 3 and 15 s shown in Figure 9. Therefore, a high concentration of nitrogen caused an imbalance between the mass flow displaced by the compressor and the mass flow entering the capillary tube, which reduced the refrigerator performance.

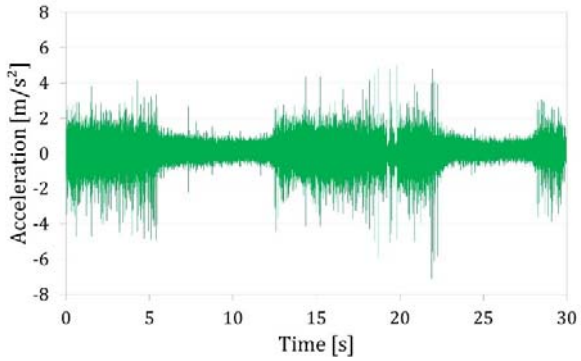

Figure 8: Acceleration data: 0.53% of nitrogen at 2500 RPM

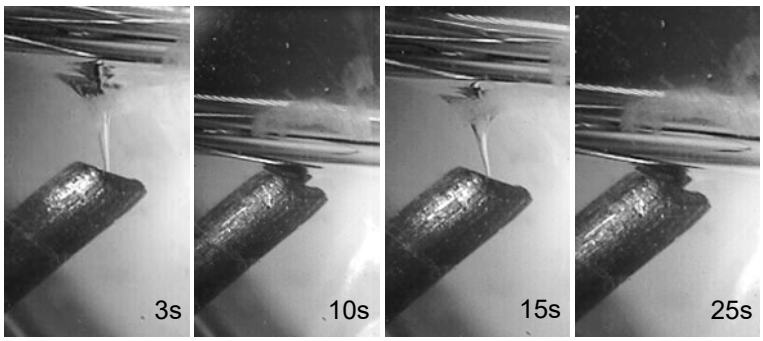

Figure 9: Filter dryer images: 0.53% of nitrogen at 2500 RPM

5. CONCLUSIONS

In this study, the effect of non-condensable gases in household refrigerators was investigated by inserting different amounts of nitrogen into the refrigeration circuit with a purpose-built accurate device. Steady-state energy consumption tests were carried out to evaluate the system performance with different nitrogen mass fractions. This methodology proved to be very good to get an insight on the system behavior when nitrogen was added, especially for directly measured variables (such as pressures and temperatures). In addition, the vibration on the tube wall caused by the internal flow was monitored by an accelerometer strategically installed at the evaporator inlet. Simultaneously, images of the flow at the capillary tube inlet were recorded by a high-speed camera using an acrylic-made filter dryer. In some cases, when the nitrogen mass fraction was very small, the system was not strongly penalized and even developed a slightly better performance. At these operating points, the capillary tube

was probably oversized, so that the entrance of a gaseous mixture increased its restriction, and the system performed better. However, when the concentration of nitrogen was too high, the system performance was negatively affected, and large fluctuations in the flow pattern could be visualized, alternating between moments with the predominance of vapor entering the expansion device and moments with the predominance of liquid. Additionally, a higher sub-cooling degree was found to be a strong evidence of the presence of non-condensable gases. Finally, it must be pointed out that since the refrigerator was tested under steady-state conditions, some effects of the on-off operation of the compressor might have been mitigated. In this context, standardized cyclic tests can show a wider view in this topic.

REFERENCES

Cecchinato, L., Dell'eva, M., Fornasieri, E., Marcer, M., Monego, O. & Zilio, C. (2007). The effects of non-condensable gases in domestic appliances. *Applied T. Eng., 30*(1), 19-27.

Gonçalves, J. M., Melo, C. & Vieira, L. A. T. (2000). Estudo experimental de um refrigerador no-frost. Parte I: Transferência de calor através das paredes. *Proceedings of the 1st National Congress of Mechanical Engineering*. Natal, RN, Brazil: ABCM. (in Portuguese)

Gonçalves, J. M. (2004). Desenvolvimento e Aplicação de uma Metodologia para a Análise Térmica de Refrigeradores Domésticos. P.hD. thesis, Federal University of Santa Catarina, Florianópolis, Brazil. (in Portuguese)

Hermes, C. J. L., Melo, C. & Knabben, F. T. (2013). Alternative test method to assess the energy performance of frost-free refrigerating appliances. *Applied T. Eng., 50*(1), 1029-1034.

ACKNOWLEDGEMENTS

This study was made possible through the financial funding from the EMBRAPII Program (POLO/UFSC EMBRAPII Unit - Emerging Technologies in Cooling and Thermophysics). The authors thank Whirlpool S.A. for financial and technical support. The authors also thank Jean R. Backer, André A. Furlan and Arthur S. A. Marcon for their help with the experiments.